Journal of Materials Chemistry

Cite this: J. Mater. Chem., 2012, 22, 10303

www.rsc.org/materials

PAPER

Structural flexibility and intrinsic dynamics in the $M_2(2,6\text{-ndc})_2(dabco)$ (M = Ni, Cu, Co, Zn) metal–organic frameworks†

Nicole Klein,[a] Herbert C. Hoffmann,[ab] Amandine Cadiau,[a] Juergen Getzschmann,[a] Martin R. Lohe,[a] Silvia Paasch,[b] Thomas Heydenreich,[b] Karim Adil,[c] Irena Senkovska,[a] Eike Brunner*[b] and Stefan Kaskel*[a]

Received 1st November 2011, Accepted 8th February 2012
DOI: 10.1039/c2jm15601f

The synthesis and structural flexibility of the metal–organic frameworks $M_2(2,6\text{-ndc})_2(dabco)$ (DUT-8(M), M = Ni, Co, Cu, Zn; 2,6-ndc = 2,6-naphthalenedicarboxylate, dabco = 1,4-diazabicyclo[2.2.2] octane) as well as their characterization by gas adsorption, ^{129}Xe NMR and ^{13}C MAS NMR spectroscopy are described. Depending on the integrated metal atom the compounds show reversible (DUT-8(Ni), DUT-8(Co)), non-reversible (DUT-8(Zn)) or no (DUT-8(Cu)) structural transformation upon solvent removal and/or physisorption of several gases. DUT-8(Co) exhibits a similar structural transformation by solvent removal and adsorption behavior as observed for DUT-8(Ni). DUT-8(Zn) undergoes an irreversible structural change caused by solvent removal. The non-flexible copper containing MOF reveals the best performance concerning porosity and gas storage capacities within the DUT-8 series. Xenon adsorption studies combined with ^{129}Xe NMR spectroscopy are used to study the flexibility of the DUT-8 compounds. ^{129}Xe chemical shift and line width strongly depend on the metal atom. Solid-state ^{13}C NMR spectroscopy has been applied in order to further characterize the organic parts of the DUT-8 frameworks. While DUT-8(Ni) exhibits narrow, well-resolved lines in its "as made" state, the signals of DUT-8(Co) are broadened and shifted over an unusually wide chemical shift range (−72 to 717 ppm). No detectable signals are found in DUT-8(Cu) indicating significantly changed internal dynamics compared to DUT-8(Ni) and DUT-8(Co).

Introduction

Porous metal–organic frameworks (MOFs) are currently under intensive investigation because of their rich structural chemistry and outstanding properties, regarding not only the specific surface area and storage capacities, but also the flexibility of the framework. In recent years, several examples of MOFs which are capable of performing reversible structural transformations as a response to external stimuli such as gas or liquid adsorption/desorption have been reported.[1] Dynamic structural transformation based on flexible crystalline coordination polymers is one of the most interesting phenomena. This effect is rarely observed in established porous materials such as zeolites and activated carbons.

The guest molecules hosted in the pores of such MOFs are often directing the structural transformation. Selective removal or exchange of the guests drives the reversible dynamic behavior of the network often described as breathing. This behavior can be compared with biological systems. For example, in aerobic organisms the heme molecule changes its protein folding in response to partial gas pressures and the selectivity to O_2 *vs.* CO_2 can be achieved in such a way.

So far the predictability of flexible systems is still limited. In their pioneering work, Kitagawa *et al.* have successfully developed flexible architectures using rational concepts.[2] Models describing the thermodynamics of adsorption-induced topotactic transformation have been developed recently.[3,4] However, the structural transformations in MIL-53 are more complex due to the presence of hydrogen bonding interactions.[1,5] The systematic investigation of the adsorptive and dynamic properties of isotypic materials with different metal nodes or different functionalities of the organic linker can bring forward the understanding of factors, which are crucial for the modular synthesis of flexible coordination polymers. Recently, Fischer *et al.* have shown that the functionalization of MOF-5 ($Zn_4O(1,4\text{-bdc})_3$, 1,4-bdc = 1,4-benzenedicarboxylate), which is known to be a rigid framework,

[a]*Department of Inorganic Chemistry, Dresden University of Technology, Bergstr. 66, D-01069 Dresden, Germany. E-mail: stefan.kaskel@chemie.tu-dresden.de; Fax: +49 351-46337287; Tel: +49 351-46332564*
[b]*Bioanalytical Chemistry, Dresden University of Technology, Bergstr. 66, D-01069 Dresden, Germany. E-mail: Eike.Brunner@chemie.tu-dresden.de; Fax: +49 351 46337188; Tel: +49 351 463 32631*
[c]*Laboratoire des Oxydes et Fluorures, UMR CNRS 6010, Université du Maine, Avenue O. Messiaen, 72085 Le Mans Cedex 05, France. E-mail: karim.adil@univ-lemans.fr; Fax: +33 243833506; Tel: +33 243833352*
† Electronic supplementary information (ESI) available: Profile Rietveld refinement, TGA, thermodiffraction, additional PXRDs, additional adsorption measurements, magnetisation measurements, ^{129}Xe and ^{13}C NMR spectra. See DOI: 10.1039/c2jm15601f

with additional alkyl ether groups on the benzyl ring of the type $–O–(CH_2)_n–O–CH_3$ (n = 2–4) initiates unexpected structural flexibility, as well as high sorption selectivity towards CO_2 over N_2 and CH_4.[6]

Recently, we reported a nickel based pillar layer MOF (DUT-8(Ni); Ni_2(2,6-ndc)$_2$(dabco); 2,6-ndc = 2,6-naphthalenedicarboxy late, dabco = 1,4-diazabicyclo[2.2.2]octane) with pronounced flexibility of the network, reflected in large hysteresis loops by the adsorption of certain gases and changes in the powder X-ray diffraction pattern during evacuation.[7] In the case of DUT-8(Ni), ^{129}Xe NMR spectroscopy has also been proven to be a reliable tool to get a deeper insight into the breathing process. It is noteworthy that, shortly after, Lee *et al.* published a compound with the same framework composition, synthesized in a different solvent, which shows no pronounced flexible behavior and type I isotherm during nitrogen adsorption.[8]

In the M_2(2,6-ndc)$_2$(dabco) (M = Ni, Cu, Co, Zn) frameworks, the exchange of the metal is possible maintaining the network topology. Investigating the sorption properties of the MOFs we observed significant differences in the adsorption behavior corresponding to different degrees of the network flexibility. The results of crystallographic studies correspond to the adsorption isotherms, showing changes in the crystal structures during the evacuation or resolvation/adsorption. ^{129}Xe NMR as well as ^{13}C MAS NMR measurements give further information about host–guest interactions, paramagnetism and intrinsic dynamics present in the different DUT-8 compounds.

Results and discussion

The compound DUT-8(Ni) with the composition Ni_2(2,6-ndc)$_2$(dabco) shows pronounced structure flexibility during the removal or adsorption of guest molecules. Exchanging the nickel in DUT-8(Ni) with metals such as zinc, cobalt or copper, a series of M_2(2,6-ndc)$_2$(dabco) compounds (further named DUT-8(M), M = Ni, Co, Cu, Zn) could be synthesized.

Structure

Crystals, suitable for single crystal structure analysis, could not be obtained. The comparison of the powder X-ray diffraction patterns (PXRDs) of the three solvent containing DUT-8(M) (M = Co, Cu, Zn) compounds with the experimental PXRD of DUT-8(Ni) reveals some similarity (Fig. 1).

The Rietveld analysis of the DUT-8(M) (M = Co, Cu, Zn) powder patterns confirms the isotypism of these compounds with DUT-8(Ni). The structures of DUT-8(Co) and DUT-8(Cu) could be refined in the tetragonal space group *P4/n*.

The structure of DUT-8(Zn) was solved and refined in the monoclinic space group, *P2/n* (Table 1). This monoclinic cell can be derived from the tetragonal cell of DUT-8(Ni) as shown in Fig. 2.

Thus, the compounds consist of binuclear paddle wheel M_2-units bridged by four 2,6-ndc anions to 2D square-grid layers. The axial sites of the M_2-paddle wheels are coordinated by nitrogen atoms of the neutral dabco ligands (Fig. 2), connecting the 2D layers into a 3D structure with a primitive cubic (**pcu**) net topology.

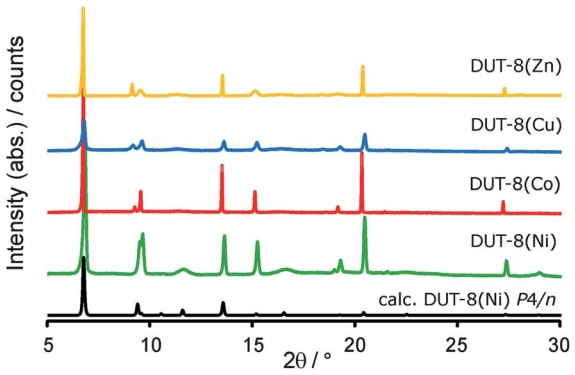

Fig. 1 PXRD patterns of the "as made" DUT-8(M) compounds: DUT-8(Ni) (green), DUT-8(Co) (red), DUT-8(Cu) (blue) and DUT-8(Zn) (yellow) in comparison with the calculated pattern of the "as made" DUT-8(Ni) (black).

Solvent removal

The thermodiffraction experiments (see ESI†, Fig. S9–S12) show that Co, Ni, and Zn containing DUT-8 compounds undergo different structural changes during solvent removal. In contrast, the structure of DUT-8(Cu) remains unchanged up to the decomposition of the sample. Fig. 3 shows the comparison of PXRD patterns of the investigated materials in the activated state and the calculated pattern of the "as made" DUT-8(Ni). It is evident that even the structural change of the activated phase of DUT-8(Ni) is different from the structural change of the activated phases of the cobalt and zinc containing compounds. It can be proposed that the solvent removal in the case of DUT-8(Co) and DUT-8(Zn) just leads to a narrowing but not "closing" of the pores in comparison to DUT-8(Ni). The resolvation experiment of the activated DUT-8(Co) phase in *N*,*N*-dimethylformamide (DMF) leads to the "as made" phase (see ESI†, Fig. S13). Thus, structural transformation of DUT-8(Co) caused by activation is completely reversible. DUT-8(Zn) shows no changes in the PXRD pattern after soaking the activated phase in DMF (see ESI†, Fig. S15). The structure of the activated phase cannot be transformed in the "as made" phase by resolvation in DMF.

For the isoreticular M_2(1,4-bdc)$_2$(dabco) compounds it is known that the zinc,[9] cobalt[10] and nickel[11] containing compounds show flexibility by exchanging or removing solvent molecules, which is not the case for the isomorphous copper phase.[12] To the best of our knowledge, no non-interpenetrated metal–organic framework is known so far, which is based on a pillar layer motif and copper-paddle-wheel units demonstrating reversible flexible behavior.

Gas adsorption

To evaluate the porosity and response of the frameworks during adsorption, carbon dioxide (Fig. 4) and nitrogen (Fig. 5) physisorption isotherms are collected at 195 K and 77 K, respectively.

As expected based on PXRD experiments, a hysteresis loop is observed during the CO_2 physisorption on DUT-8(Co). But in contrast to DUT-8(Ni), the cobalt containing compound shows significant adsorption already at low relative pressure, and the

Table 1 Crystallographic data of DUT-8(M) (M = Ni, Co, Cu, Zn)

	DUT-8(Ni)[a]	DUT-8(Co)	DUT-8(Cu)	DUT-8(Zn)
Crystal system	Tetragonal	Tetragonal	Tetragonal	Monoclinic
Space group	*P4/n*	*P4/n*	*P4/n*	*P2/n*
a/Å	18.4312(16)	18.5169(11)	18.3761(5)	18.5327(14)
b/Å	—	—	—	19.3350(5)
c/Å	9.3905(8)	9.5254(6)	9.6523(5)	18.3808(13)
β/°	—	—	—	90.053(3)
V/Å^3	3190.0(5)	3266.0(3)	3259.4(2)	6586.4(7)
Temperature/K	293	293	293	293
Wavelength/Å	—	1.54056	1.54056	1.54056
2*θ* range/°	—	3–50	2–90	3–50
Refined parameters	—	60	67	63
Nb reflexions	—	285	1540	1138
R_p R_{wp} R_{exp}	—	2.28 2.89 2.77	8.45 11.3 11.15	5.67 7.45 1.86

[a] Crystallographic data from single crystal measurement.[7]

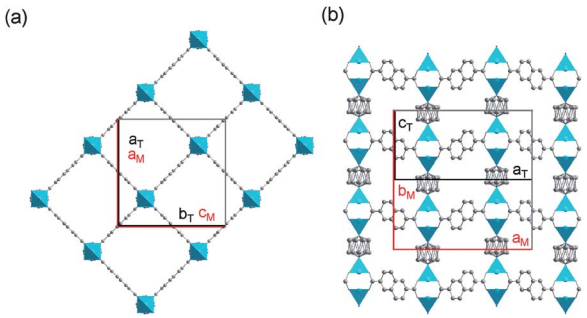

Fig. 2 (a) View along the channels of DUT-8(M) (along *b* for DUT-8(Zn) and along *c* for DUT-8(M) (M = Ni, Co, Cu)) and (b) view on the structure along *c* for DUT-8(Zn) and along *b* for DUT-8(M) (M = Ni, Co, Cu); relationship between the tetragonal cell of DUT-8(M) (M = Ni, Co, Cu) (in black, with a_T, b_T, and c_T) and the monoclinic cell of DUT-8(Zn) (in red, with a_M, b_M, and c_M) (metal: cyan, O: red, N: blue, C: grey).

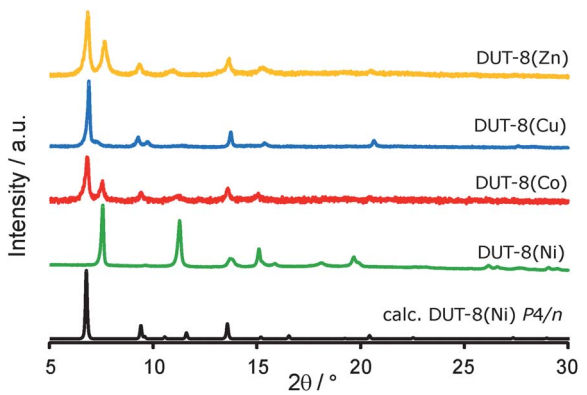

Fig. 3 PXRD patterns of activated DUT-8(M) phases (DUT-8(Ni) (green), DUT-8(Co) (red), DUT-8(Cu) (blue) and DUT-8(Zn) (yellow)) in comparison with the calculated pattern of the "as made" DUT-8(Ni) (black).

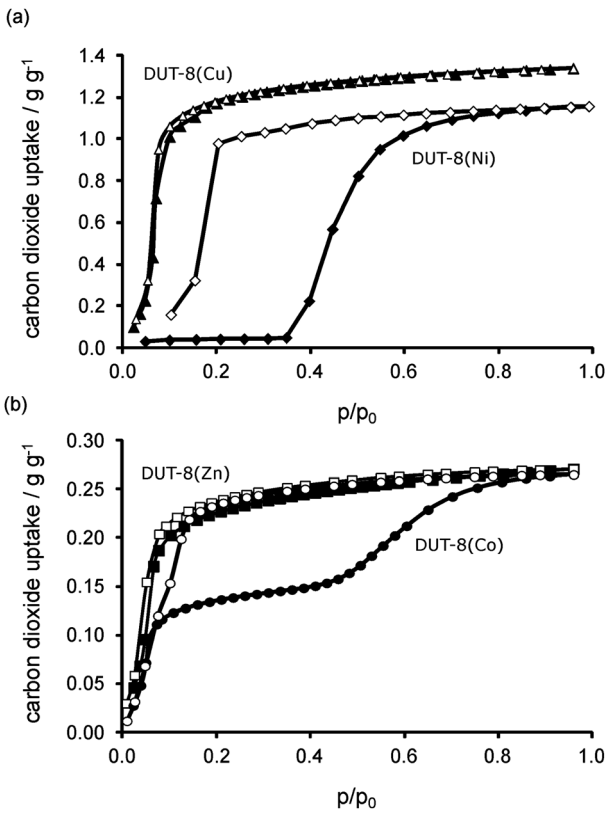

Fig. 4 Carbon dioxide adsorption (filled symbols) and desorption (empty symbols) isotherms of (a) DUT-8(Cu) (triangles), DUT-8(Ni) (diamonds) and (b) DUT-8(Zn) (squares), and DUT-8(Co) (circles), measured at 196 K.

isotherm follows type I with a second step at $p/p_0 = 0.4$. At higher relative pressure, the adsorbed amount increases again and reaches the value of 133 cm^3 g^{-1} (0.26 g g^{-1}) at $p/p_0 = 0.95$. Thus, the total CO_2 amount adsorbed is 4.5 times lower in comparison to DUT-8(Ni) (590 cm^3 g^{-1}, 1.16 g g^{-1} at $p/p_0 = 0.95$). The desorption branch does not retrace the adsorption one, generating a hysteresis loop. The hysteresis closes at $p/p_0 = 0.07$. DUT-8(Zn) shows the typical behavior for microporous materials, exhibiting the type I isotherm and an uptake similar to DUT-8(Co). It should be mentioned that the zinc based material has the poorest crystallinity after activation indicating the low stability of the compound and partial collapse of the framework. DUT-8(Cu) reaches the best uptake of 680 cm^3 g^{-1} (1.34 g g^{-1}) at $p/p_0 = 0.95$ and shows a fully reversible physisorption isotherm.

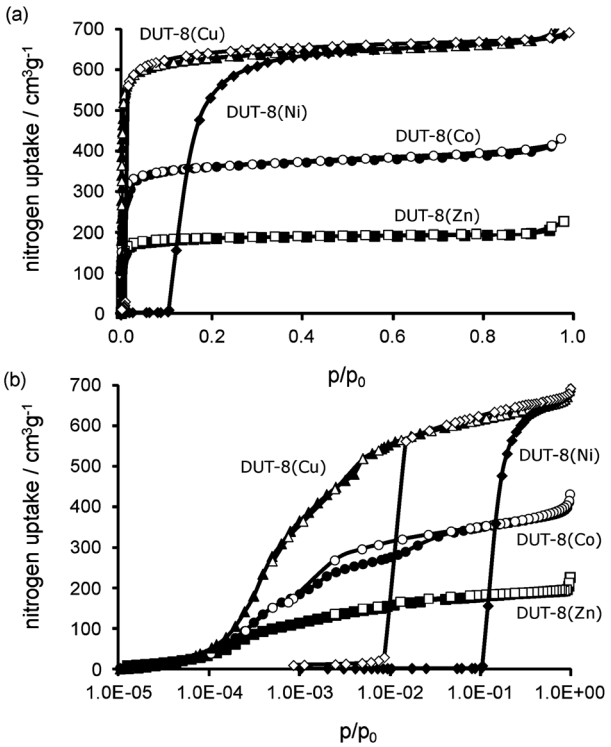

Fig. 5 Nitrogen adsorption (filled symbols) and desorption (empty symbols) isotherms of (a) DUT-8(Cu) (triangles), DUT-8(Ni) (diamonds), DUT-8(Zn) (squares) and DUT-8(Co) (circles), and (b) on a semi-logarithmic scale, measured at 77 K.

The S-shape of the isotherm is similar to that found for other MOFs with rigid frameworks.[13]

We used the CO_2 adsorption measurements to illustrate the different "closing degree" of the activated materials, as well as different "pore widening" during the adsorption.

As borderline cases the activated DUT-8(Ni) (closed structure, pore volume negligible (~4%)) and DUT-8(Cu) (fully open framework, pore volume 100%) are considered. The structure of DUT-8(Cu) is consistent and undergoes no changes during activation or adsorption.

During the CO_2 adsorption, the pore volume of DUT-8(Ni) increases from 4% up to 86%. On the other hand the pore volume of the activated cobalt containing compound amounts to 10%, which increases up to 19% after the gate-opening. For DUT-8(Zn) change in the pore volume is observed only during the activation (from 100% to 19%); this remains unchanged during the adsorption of the investigated gases (see ESI†, Fig. S4 and S5).

The N_2 adsorption at 77 K confirms the observations collected during the CO_2 adsorption experiments. In the case of N_2 adsorption, a less pronounced hysteresis effect is observed for DUT-8(Co) and the gate-opening pressure is shifted to lower values in comparison to DUT-8(Ni). Nitrogen adsorption starts already at low pressures as indicated by a steep rise of the adsorption branch. At the relative pressure of 2×10^{-3}, a first plateau is reached followed by a second step in the isotherm at $p/p_0 = 10^{-2}$. In this relative pressure range the desorption branch does not trace the adsorption branch giving a small hysteresis loop. For DUT-8(Cu) and DUT-8(Zn), type I isotherms are observed, and DUT-8(Cu) has the highest nitrogen uptake of 670 $cm^3\ g^{-1}$ (Fig. 5). The total nitrogen uptake of the cobalt containing phase with 400 $cm^3\ g^{-1}$ and the zinc phase with 200 $cm^3\ g^{-1}$ is significantly lower compared to DUT-8(Cu) and DUT-8(Ni) (Fig. 5). The differences in the total nitrogen uptake are obviously caused by the different degrees of flexibility and stability of the compounds.

The BET surface areas calculated from the adsorption branch and total pore volumes are: 2535 $m^2\ g^{-1}$ and 1.04 $cm^3\ g^{-1}$ for DUT-8(Cu), 1400 $m^2\ g^{-1}$ and 0.62 $cm^3\ g^{-1}$ for DUT-8(Co) and 710 $m^2\ g^{-1}$ and 0.30 $cm^3\ g^{-1}$ for DUT-8(Zn).

The *n*-butane adsorption experiments are performed at 293 K under atmospheric pressure and dynamic conditions (Fig. 6). According to the measurements, the best performance regarding the storage capacity was obtained for DUT-8(Cu) (0.43 g g^{-1}), followed by DUT-8(Ni) (0.34 g g^{-1} in the open state). The DUT-8(Zn) and DUT-8(Co) have significantly lower, comparable uptake (0.10 g g^{-1} and 0.12 g g^{-1}, respectively). Interestingly, for all compounds with the exception of DUT-8(Ni), no gate-pressure effect could be observed under the investigated conditions.

The low pressure adsorption measurements confirm the assumption of different degrees of structural changes caused by solvent removal and insertion of gas molecules in the DUT-8 series. The activated phases of DUT-8(Co) and DUT-8(Zn) seem to be between the "open" and "closed" state and therefore accessible for guest molecules already at low relative pressures. DUT-8(Zn) shows no hysteresis loop for any investigated adsorbate and therefore probably no structural changes during the adsorption of those gases.

As reported before, DUT-8(Ni) adsorbs only small amounts of hydrogen even at high pressures and 77 K.[7] To compare the hydrogen storage capacities, hydrogen physisorption isotherms up to 100 bar were measured for all isotypic DUT-8 compounds at 77 K (Fig. 7a, for the hydrogen uptake up to 1 bar see Fig. S16 in the ESI†). DUT-8(Cu) has the highest hydrogen excess storage capacity within the DUT-8 series with 4.27 wt% (44.6 mg g^{-1}) at 35 bar and 77 K. DUT-8(Co) and DUT-8(Zn) have a hydrogen uptake of 2.91 wt% (30 mg g^{-1}) at 35 bar and 1.19 wt% (12 mg g^{-1}) at 26 bar and 77 K.

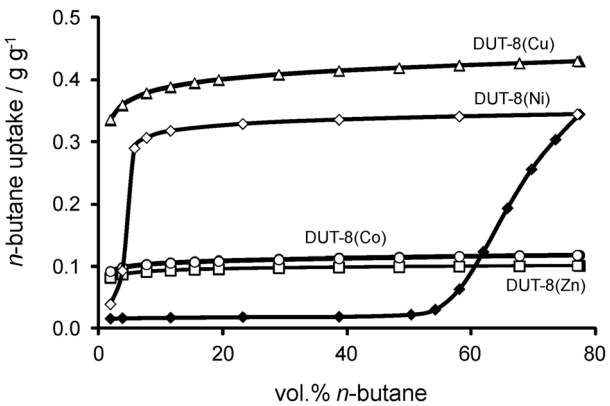

Fig. 6 *n*-Butane adsorption (filled symbols) and desorption (empty symbols) isotherms of DUT-8(Cu) (triangles), DUT-8(Ni) (diamonds), DUT-8(Co) (circles) and DUT-8(Zn) (squares) at 293 K.

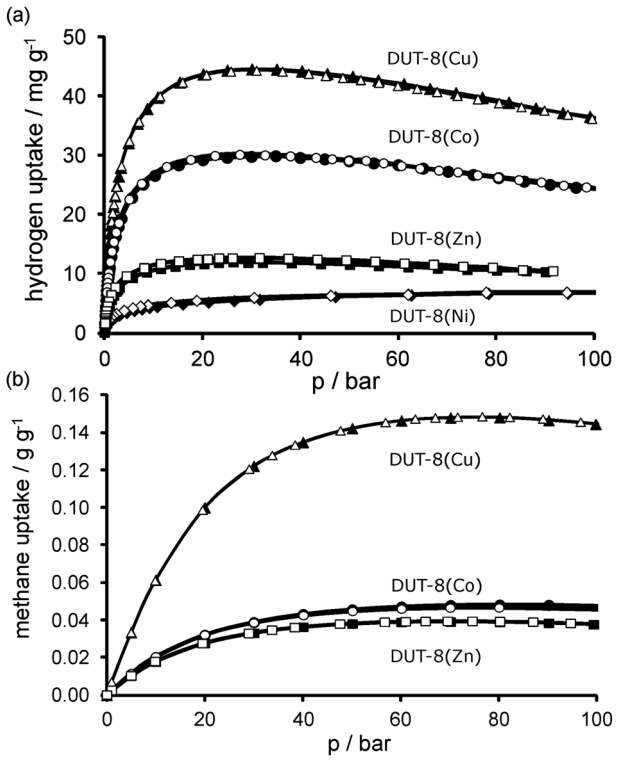

Fig. 7 High pressure excess adsorption isotherms of (a) hydrogen (77 K) and (b) methane (298 K); DUT-8(Cu) (triangles), DUT-8(Ni) (diamonds), DUT-8(Zn) (squares), DUT-8(Co) (circles).

These values are comparable with other microporous materials, *e.g.* $Cu_3(btc)_2$ (3.6 wt%, 50 bar),[14] the non-flexible Ni_2(2,6-ndc)$_2$(dabco) phase published by Lee *et al.* (5.5 wt%, 65 bar)[8] or the M_2(1,4-bdc)$_2$(dabco) (M = Zn, Co, Cu, Ni) series with 3.07 wt% at 40 bar for Zn_2(1,4-bdc)$_2$(dabco), 3.95 wt% at 40 bar for Co_2(1,4-bdc)$_2$(dabco), 2.63 wt% at 40 bar for Cu_2(1,4-bdc)$_2$(dabco) and 3.96 wt% at 28.1 bar for the Ni_2(1,4-bdc)$_2$(dabco).[15,16]

Methane excess adsorption isotherms up to 120 bar were measured at 298 K using a magnetic suspension balance (Fig. 7b). DUT-8(Cu) reaches the highest maximum uptake of 148 mg g^{-1} (at 76 bar and 298 K). This value is comparable to the M_2(1,4-bdc)$_2$dabco (M = Co, Zn) compounds and $Cu_3(btc)_2$.[10,17] The zinc and cobalt containing MOFs have significantly lower adsorption capacity of approximately 45 mg g^{-1}.

For the nickel containing DUT-8 compound high pressure nitrogen, oxygen, methane and carbon dioxide adsorption isotherms at 298 K up to 50 bar were measured.[7] The high pressure CO_2 isotherm measured at room temperature (RT) shows a comparable pronounced gate-pressure effect as in the isotherm measured at 196 K (Fig. 4). However, the uptake of N_2, O_2 and CH_4 is very low under the investigated conditions. Therefore the application for separation of CO_2 from CH_4 at high pressures can be considered. The CO_2 isotherms for DUT-8(Cu) and DUT-8(Zn) samples show no hysteresis loop (see ESI†, Fig. S17). The copper containing compound has the highest storage capacity within the DUT-8 series. DUT-8(Cu) has an uptake of 0.76 g g^{-1} at 50 bar, followed by DUT-8(Ni) (0.68 g g^{-1}) and DUT-8(Zn) (0.23 g g^{-1}).

^{129}Xe NMR spectroscopy

Xenon adsorption studies combined with ^{129}Xe NMR spectroscopy are favorable methods for the characterization of porous materials[18–29] and can be used to study the so-called gate-pressure effect in the flexible MOF materials.[7,30–32]

Recently, we have used high-pressure *in situ* ^{129}Xe NMR spectroscopy in order to study DUT-8(Ni).[31] One major observation was the appearance of a narrow signal at relatively high ^{129}Xe chemical shift (*ca.* 220–230 ppm) due to xenon adsorbed inside the pore system of DUT-8(Ni) in its open state. It was concluded that this chemical shift is strongly influenced by xenon–xenon interactions and indicates the formation of an almost liquid-like xenon phase inside the MOF after the pressure induced pore-opening.[31] Furthermore, a paramagnetic shift of the order of 20 ppm may also contribute to the high chemical shift value observed for ^{129}Xe in DUT-8(Ni).

Within the present paper, high-pressure *in situ* ^{129}Xe NMR spectroscopy was also applied to DUT-8(Cu) and DUT-8(Co). The DUT-8(Cu) framework is always open even in the activated state, *i.e.*, it does not show any gate-pressure effect. In contrast, DUT-8(Co) undergoes a structural change during solvent removal and exhibits a gate-pressure effect as observed previously for DUT-8(Ni). However, DUT-8(Ni) shows a very pronounced hysteresis in the xenon adsorption isotherm at 165 K in contrast to DUT-8(Co) which exhibits a very weak hysteresis only (Fig. 8). So the results of the ^{129}Xe NMR investigations correspond well to the adsorption measurements described above. Insofar, comparative ^{129}Xe NMR studies of DUT-8(M) (M = Ni, Co, Cu) are particularly interesting.

Fig. 9a shows the ^{129}Xe NMR spectra of activated DUT-8(Cu) as a function of xenon pressure at room temperature. Apart from the gas phase signal, a signal with a strongly pressure-dependent chemical shift occurs which can be ascribed to xenon adsorbed inside the pore system of DUT-8(Cu). This observation agrees with the above described adsorption studies indicating that the pore system of DUT-8(Cu) is always open. The observed pressure-dependence of the chemical shift (see Fig. 9b) agrees with the general behavior observed previously for zeolites.[18,22] Increasing pressure results in a growing amount of adsorbed xenon inside the pore system (see also ESI†, Fig. S20) which is accompanied by increasingly strong xenon–xenon interactions

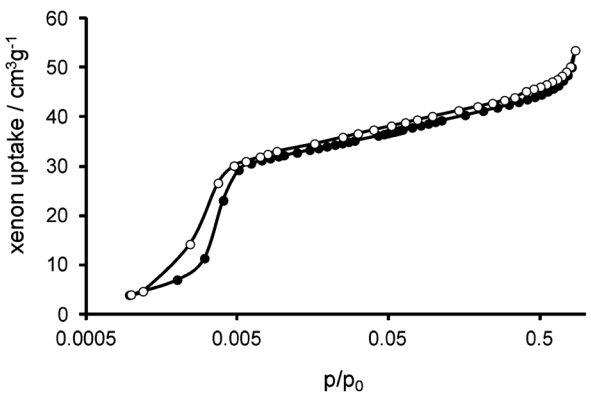

Fig. 8 Xenon adsorption (filled symbols) and desorption (empty symbols) isotherm of DUT-8(Co) at 165 K (semi-logarithmic scale).

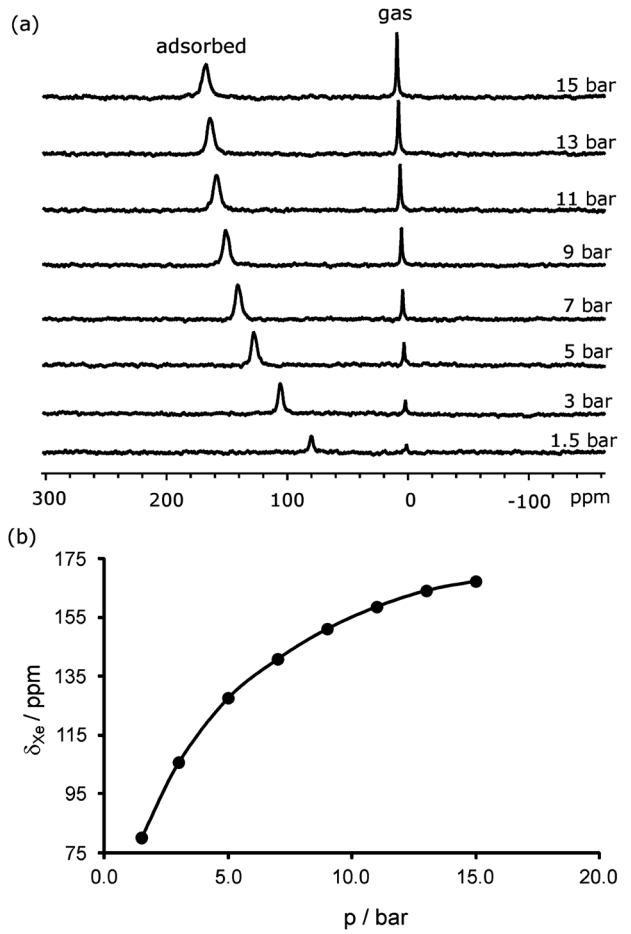

Fig. 9 (a) ^{129}Xe NMR spectra of xenon adsorbed at RT onto DUT-8(Cu) as a function of xenon pressure. (b) ^{129}Xe NMR chemical shift of the signal due to xenon adsorbed onto DUT-8(Cu) at RT. Note that the xenon chemical shift observed at stepwise increasing pressures (adsorption) exactly corresponds to shifts measured afterwards at stepwise decreasing pressures (desorption).

giving rise to higher chemical shifts. At 15 bar and RT, the chemical shift of adsorbed xenon amounts to 168 ppm. The chemical shift of this signal further increases at decreasing temperature (see ESI†, Fig. S19). It is, furthermore, important to note that the spectra obtained during the initial stepwise pressure increase (adsorption experiment) exhibit identical chemical shifts and signal intensities as observed after applying a certain maximum pressure and subsequent pressure release (desorption experiment). In other words, absolutely no hysteresis between the xenon adsorption and desorption behavior is observed for DUT-8(Cu) in contrast to DUT-8(Ni) (see Fig. 9b and S20†).

The spectrum of DUT-8(Co) only exhibits a gas phase signal at xenon pressures up to 17.4 bar and 245 K (see Fig. 10), *i.e.*, the pore system remains closed even at this relatively high pressure and low temperature. However, the pore system starts to open at 17.6 bar as can be seen from the appearance of a relatively broad signal at *ca.* 210 ppm. Pressure release shows that this signal disappears below 16.4 bar. That means, high-pressure *in situ* xenon adsorption confirms the presence of a gate-pressure effect in DUT-8(Co). Structure closing upon pressure release occurs only about 1 bar below the gate-opening pressure, *i.e.*, DUT-

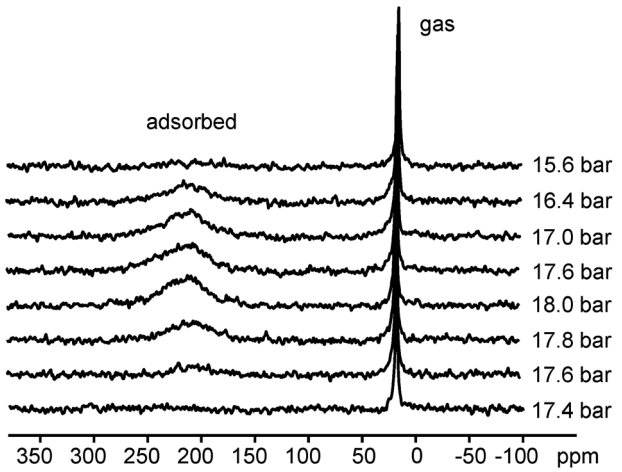

Fig. 10 ^{129}Xe NMR spectra of xenon adsorbed at 245 K onto DUT-8(Co) as a function of pressure.

8(Co) exhibits a much less pronounced hysteresis than DUT-8(Ni) as confirmed by the xenon adsorption isotherm measured at 165 K (Fig. 8).

It is interesting to note that xenon atoms adsorbed in the pore systems of DUT-8(Cu) and DUT-8(Co) exhibit similarly high chemical shift values as observed previously for DUT-8(Ni) at 15 bar and 237 K (see Fig. 11). However, the line widths are different: DUT-8(Cu) exhibits the narrowest signal with 11 ppm full width at half-maximum (FWHM). The FWHM of ^{129}Xe adsorbed in DUT-8(Ni) amounts to 17 ppm. The largest value of *ca.* 35 ppm is found for DUT-8(Co). Note that this tendency may reflect the increasingly strong paramagnetism of the different compounds. The paramagnetic susceptibilities χ within the DUT-8-family follow the order: $\chi_{DUT\text{-}8(Cu)} < \chi_{DUT\text{-}8(Ni)} < \chi_{DUT\text{-}8(Co)}$ (see ESI†, Fig. S18). As expected from this trend, the copper-containing compound indeed exhibits the lowest chemical shift. Unexpectedly, the chemical shift of xenon in DUT-8(Co) is slightly lower than in DUT-8(Ni). This is, however, not necessarily a contradiction. It is possible that the

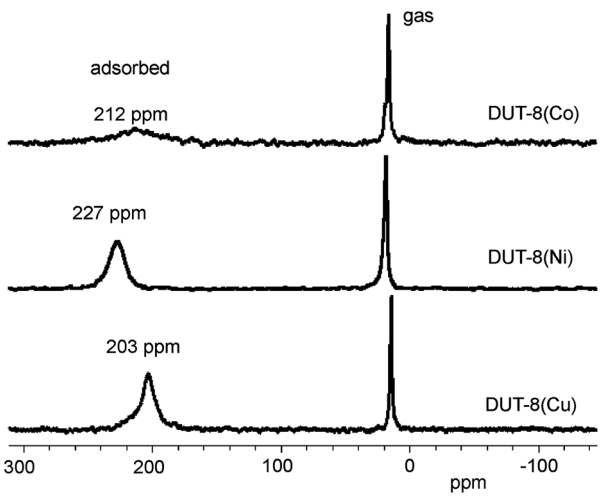

Fig. 11 ^{129}Xe NMR spectra of xenon adsorbed onto DUT-8(M), M = Cu, Ni, Co, at 237 K and 15 bar.

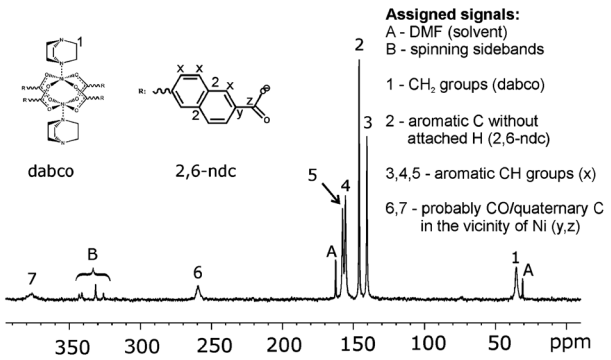

Fig. 12 ^{13}C CP MAS NMR spectrum of "as made" DUT-8(Ni) measured at RT with a sample spinning rate of 14 kHz.

paramagnetic cobalt sites preferentially act as relaxation agents for xenon causing the observed broad ^{129}Xe NMR signal rather than as shift agents—in contrast to nickel.

Solid-state ^{13}C NMR spectroscopy

Solid-state ^{13}C NMR spectroscopy has been applied in order to further characterize the compounds of the DUT-8 family. Fig. 12 shows the ^{13}C CP MAS NMR spectrum of "as made" DUT-8(Ni). The spectrum exhibits seven well-resolved, narrow lines apart from the signals due to the solvent DMF. In order to assign the former signals, 2D HETCOR (heteronuclear correlation spectroscopy) and APT (attached proton test)[33] experiments have been performed. The ^{1}H–^{13}C HETCOR spectrum measured with a short contact time (200 μs) is shown in Fig. 13. At this short contact time, signals of carbon atoms with directly attached ^{1}H will preferentially be detected. That means, the signals at 141, 156, and 158 ppm can be attributed to the ^{13}C atoms *X* corresponding to signals 3–5 in the aromatic rings with directly attached ^{1}H. Furthermore, a signal at 35 ppm is observed in the 2D HETCOR which can be attributed to the CH_2 groups in dabco (signal 1 in Fig. 12). Signal 2 observed at 146 ppm for a mixing time of 4000 μs is absent in the 2D HETCOR measured at short mixing time. That means, it is caused by carbon atoms in the position denoted by 2 in Fig. 12. These carbon atoms in the aromatic rings do not exhibit directly attached ^{1}H nuclei. The signals 6 and 7 which were observed in the CP spectra at longer mixing times at chemical shifts of 260 and 376 ppm are absent at short mixing times. This observation in combination with the unusually high chemical shifts indicates that signals 6 and 7 are likely to be due to carbons in the positions *y* and *z* close to Ni (*cf.* Fig. 12).

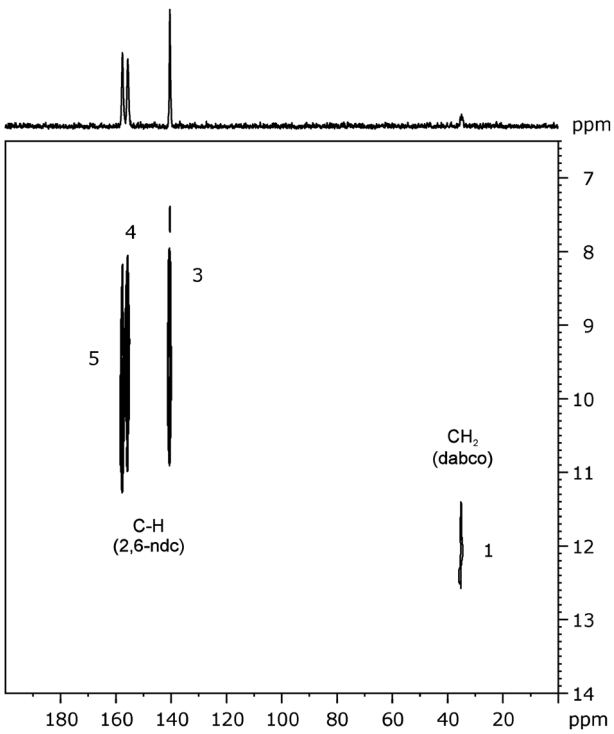

Fig. 13 two-dimensional ^{1}H–^{13}C HETCOR spectrum of "as made" DUT-8(Ni) measured at RT with a contact time of 200 μs and with a 14 kHz sample spinning rate.

In contrast to DUT-8(Ni), the copper-containing compound DUT-8(Cu) does not exhibit observable ^{13}C NMR signals. Both, directly ^{13}C excited as well as ^{13}C CP NMR spectra only exhibit the narrow lines due to DMF (see Fig. 14). These signals are more intense in the directly excited spectrum. That means, the ^{13}C–^{1}H CP efficiency is relatively low, probably due to the mobility of DMF molecules inside the pore system. The absence of any signal due to 2,6-ndc and dabco is surprising because DUT-8(Cu) is less paramagnetic than DUT-8(Ni). It is, therefore, likely that the absence of these ^{13}C NMR signals is due to dynamic effects and/or static disorder. Static disorder seems to be rather unlikely since the diffraction patterns (see Fig. 3 and S14†) confirm the crystallinity of the sample. It seems, therefore, likely that local thermal motions are responsible for this effect. Thermal motions at a time scale of the order of the inverse sample spinning rate[34–37] may result in a considerable line broadening making the signals undetectable—not only in the CP but also in the directly excited spectra. Furthermore, the CP efficiency will be low in such cases.[38] Since the overall structure and porosity of the material remain intact despite these local motions, ^{129}Xe NMR detects the pores of the framework (see Fig. 9 and 11). Moreover, small structural variations can further contribute to the line width. Finally, the influence of

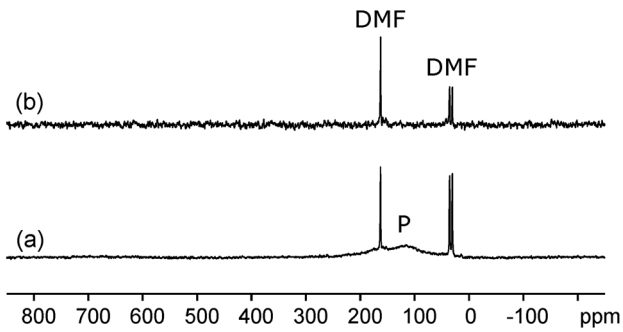

Fig. 14 Directly (a) ^{13}C excited as well as (b) ^{13}C CP MAS NMR spectrum of "as made" DUT-8(Cu) measured at RT with sample spinning rates of 16 kHz. P denotes the broad signal due to the probe and is not related to the sample.

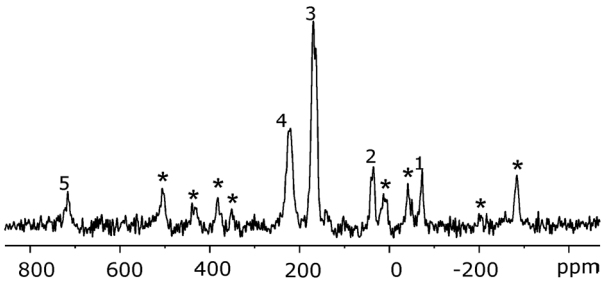

Fig. 15 ^{13}C CP MAS NMR spectrum of "as made" DUT-8(Co) measured at RT with a sample spinning rate of 16 kHz. Chemical shifts of the identified signals: 1: 72 ppm; 2: 38 ppm; 3: 168 ppm; 4: 223 ppm; and 5: 717 ppm. *: denotes spinning sidebands. The signals 2 and 3 are also caused by DMF.

paramagnetic sites cannot be ruled out completely—although it is expected to be smaller than in DUT-8(Ni).

The ^{13}C CP MAS NMR spectrum of DUT-8(Co) is shown in Fig. 15. Although this compound exhibits the highest paramagnetic susceptibility, ^{13}C NMR signals are clearly detected in contrast to DUT-8(Cu). These signals are, however, considerably broader than in DUT-8(Ni). Some of these signals occur at very unusual positions (717 ppm, −72 ppm). Both observations are likely to be due to the influence of the paramagnetic cobalt sites. In analogy to these observations, unusual ^{13}C NMR chemical shifts were also reported for other paramagnetic MOFs.[39]

Conclusions

The present work shows a further example for different flexibility degrees of a given network topology depending on the integrated metal atom. We were able to synthesize three materials isotype to the previously reported highly flexible Ni_2(2,6-ndc)$_2$(dabco) (DUT-8(Ni)). The cobalt containing compound shows behavior similar to DUT-8(Ni) concerning solvent removal, resolvation and gas adsorption experiments. In contrast, DUT-8(Cu) shows no flexibility, neither by solvent removal nor by adsorption of several gases. An irreversible structural transformation during solvent removal was observed for the DUT-8(Zn) phase. It shows a type I isotherm for N_2 (at 77 K), CO_2 (at 196 K) and *n*-butane (at 293 K) and therefore no flexibility during adsorption. All DUT-8(M) phases are microporous materials with specific surface areas and total pore volumes up to 2535 $m^2\ g^{-1}$ and 1.04 $cm^3\ g^{-1}$ for DUT-8(Cu). Within the DUT-8 series the copper containing material shows the highest gas storage capacities for hydrogen (4.27 wt% at 35 bar and 77 K), methane (148 mg g^{-1} at 76 bar and 298 K) and *n*-butane (0.43 g g^{-1} at 293 K).

The ^{129}Xe NMR spectra are in good agreement with the results of the adsorption experiments: the choice of the metal atom has a distinct influence upon the flexibility of the framework. While DUT-8(Ni) exhibits a gate-pressure effect which is accompanied by a pronounced hysteresis, DUT-8(Cu) is always in an open state. The ^{129}Xe NMR parameters of xenon adsorbed in DUT-8(Cu), therefore, show a similar behavior as usually found for zeolites and other rigid porous materials. The chemical shift of adsorbed xenon strongly depends on the applied xenon pressure as well as on the temperature. The open state of DUT-8(Cu) is independent of parameters like activation, temperature and pressure, at least for the studied parameter space. DUT-8(Co) exhibits a gate-pressure effect for xenon but only a very small hysteresis. The metal atom not only influences the flexibility, but also parameters like the ^{129}Xe chemical shift and the line widths. We assume that these observations could be explained by paramagnetism which is very different for DUT-8(Ni), DUT-8(Cu), and DUT-8(Co). With respect to the solid-state NMR experiments, it can also be stated that the choice of the metal atom has a pronounced influence upon the solid-state ^{13}C NMR spectra of DUT-8(M): DUT-8(Ni) exhibits well resolved, narrow ^{13}C NMR signals despite the presence of paramagnetic nickel sites. The signals in the cobalt-containing compound are significantly broadened and strongly shifted but still detectable. In contrast, no detectable ^{13}C NMR signals due to the framework of DUT-8(Cu) are found although the paramagnetic susceptibility of the copper-containing compound is lower than that of DUT-8(Ni) and DUT-8(Co). This observation probably indicates the presence of dynamics and/or intrinsic disorder in DUT-8(Cu).

Experimental section

Synthesis of M_2(2,6-ndc)$_2$(dabco)

Zn_2(2,6-ndc)$_2$(dabco). All reactants were dissolved separately: $Zn(NO_3)_2 \cdot 4H_2O$ (0.275 g, 1.05 mmol) in 5 cm^3 DMF, 2,6-H_2ndc (0.227 g, 1.05 mmol) in 15 cm^3 DMF, and dabco (0.059 g, 0.525 mmol) in 5 cm^3 DMF. The mixture was sonicated for 10 min, transferred into a Teflon vessel (50 cm^3) and heated in an autoclave at 393 K for 48 h. After cooling to RT the air-sensitive product was isolated by decanting the mother liquor and washed with fresh DMF. The resulting solid was filtered in argon flow and evacuated overnight at 353 K.

Yield: 547 mg, 75% (based on 2,6-H_2ndc).

Elemental analysis: found: C, 53.8 ± 0.6; H, 4.15 ± 0.04; O, 20.7 ± 0.3; N, 4.4 ± 0.09; Zn, 18.2 ± 0.2; calc. for $C_{30.6}H_{26.4}O_{8.7}N_{2.2}Zn_2$ [Zn_2(2,6-ndc)$_2$(dabco)(DMF)$_{0.2}$(H_2O)$_{0.5}$] C, 52.89; H, 3.83; O, 20.03; N, 4.43; Zn, 18.82%.

Co_2(2,6-ndc)$_2$(dabco). All reactants were dissolved separately: $Co(NO_3)_2 \cdot 6H_2O$ (0.201 g, 0.7 mmol) in 5 cm^3 *N*,*N*-diethylformamide (DEF), 2,6-H_2ndc (0.149 g, 0.7 mmol) in 15 cm^3 DEF and dabco (0.050 g, 0.45 mmol) in 5 cm^3 DEF. The mixture was sonicated for 10 min, transferred into a Teflon vessel (50 cm^3) and heated in an autoclave at 393 K for 48 h. After cooling to RT the air-sensitive product was isolated by decanting the mother liquor and washed with fresh DMF. The resulting solid was filtered in argon flow and evacuated overnight at 373 K.

Yield: 459 mg, 92% (based on 2,6-H_2ndc).

Elemental analysis: found: C, 54.3 ± 0.4; H, 4.1 ± 0.2; O, 21.2 ± 0.2; N, 4.65 ± 0.06; Co, 16.87 ± 0.05; calc. for $C_{31.5}H_{29.5}O_{9.5}N_{2.5}Co_2$ [Co_2(2,6-ndc)$_2$(dabco)(DEF)$_{0.5}$(H_2O)]: C, 53.69; H, 4.37; O, 20.91; N, 4.82; Co, 16.21%.

Cu_2(2,6-ndc)$_2$(dabco). All reactants were dissolved separately: $Cu(NO_3)_2 \cdot 3H_2O$ (0.338 g, 1.4 mmol) in 5 cm^3 DEF, 2,6-H_2ndc (0.303 g, 1.4 mmol) in 15 cm^3 DEF and dabco (0.078 g, 0.7 mmol) in 5 cm^3 DEF. The gel-like mixture was sonicated for 10 min, transferred into a Teflon vessel (50 cm^3) and heated in an autoclave at 393 K for 48 h. After cooling to RT the air-sensitive product was isolated by decanting the mother liquor and washed with fresh DMF. The resulting solid was filtered in argon flow and evacuated overnight at 393 K.

Yield: 576 mg, 60% (based on 2,6-H_2ndc).

Elemental analysis: found: C, 52.2 ± 0.2; H, 3.85 ± 0.12; O, 20.89 ± 0.05; N, 4.4 ± 0.03; Co, 18.8 ± 0.3; calc. for $C_{30}H_{26}O_9N_2Cu_2$ [Cu_2(2,6-ndc)$_2$(dabco)(H_2O)]: C, 52.55; H, 3.82; O, 21.0; N, 4.09; Cu, 18.54%.

Powder X-ray diffraction

The thermodiffraction experiments were performed on an X'pert pro PANalytical diffractometer (CuKα_1) for all DUT-8(M) compounds (step size: 0.017°). Powder X-ray diffraction data of the "as made" phases for the Rietveld refinement and of the activated samples were collected on a STADIP diffractometer with Cu-Kα_1 radiation ($\lambda = 1.5405$ Å) (step size: 0.1°, duration of exposure: 30 s per step) at RT. The PXRD patterns of the "as made" samples are first analyzed by the program package WinXPOW[40] and the cell parameters were refined by a whole powder pattern fit using the Le Bail method[41] in the FullProf 65 software.[42]

CCDC 869355–869357 contain the supplementary crystallographic data for this paper. These data can be obtained free of charge from the Cambridge Crystallographic Data Centre *via* www.ccdc.cam.ac.uk/data_request/cif.

Adsorption measurements

Nitrogen and hydrogen adsorption measurements up to 1 bar at 77 K were carried out using a Quantachrome Autosorb1C apparatus. The BET surface areas are estimated in the relative pressure range of $10^{-3} \leq p/p_0 \leq 4 \times 10^{-1}$ for DUT-8(Cu), $10^{-2} \leq p/p_0 \leq 10^{-1}$ for DUT-8(Co) and $10^{-3} \leq p/p_0 \leq 10^{-1}$ for DUT-8(Zn) and the total pore volumes at $p/p_0 = 0.9$. For xenon adsorption the Quantachrome Autosorb1C apparatus was extended by a cryostat from Oxford Instruments to perform the measurement up to 1 bar at 165 K. For carbon dioxide adsorption the Quantachrome Autosorb1C apparatus was extended by a Dewar vessel containing a freezing mixture of carbon dioxide snow and acetone to perform the measurement up to 1 bar at 195 K. High pressure H_2 adsorption measurements at 77 K up to 110 bar were performed using a volumetric BELSORP-HP apparatus. High pressure CH_4 adsorption was studied using a magnetic suspension balance (Rubotherm). Adsorption measurement of *n*-butane was performed with a micro-balance (B111, Setaram) at 293 K and atmospheric pressure under dynamic conditions (*n*-butane diluted with nitrogen). High purity gases were used: N_2: 99.999%, H_2: 99.999%, CH_4: 99.5%, CO_2: 99.995%, O_2: 99.999%, Xe: 99.99%, *n*-C_4H_{10}: 99.95%. For all adsorption measurements the sample were activated in vacuum (10^{-3} mbar) at higher temperatures (DUT-8(Zn): 353 K, DUT-8(Co): 373 K, and DUT-8(Cu): 393 K) for about 12 h.

^{129}Xe NMR and solid-state NMR experiments

^{129}Xe NMR measurements were performed using a novel high-pressure *in situ* apparatus as described previously.[31] The ^{129}Xe NMR spectra were measured on a Bruker Avance 300 spectrometer at a resonance frequency of 83.03 MHz using a 10 mm HR probe.

Solid-state ^{13}C NMR spectroscopic experiments were also performed on the Bruker Avance 300 spectrometer using a commercial double-resonance 2.5 mm MAS NMR probe. The samples were filled into the rotor under argon atmosphere. SPINAL24 decoupling was applied during signal acquisition.[43]

Acknowledgements

The authors are grateful for the financial support of German Research Foundation (SPP 1362) and the Helmholtz Centre Berlin (BESSY II). Special thanks go to Laura Schlechte for sample synthesis and to Dr Gudrun Auffermann (Max Planck Institute for Chemical Physics of Solids) for the performance of the elemental analyses.

Notes and references

1 G. Férey and C. Serre, *Chem. Soc. Rev.*, 2009, **38**, 1380–1399.
2 S. Bureekaew, S. Shimomura and S. Kitagawa, *Sci. Technol. Adv. Mater.*, 2008, **9**, No pp. given.
3 C. Triguero, F.-X. Coudert, A. Boutin, A. H. Fuchs and A. V. Neimark, *J. Phys. Chem. Lett.*, 2011, **2**, 2033–2037.
4 A. V. Neimark, F.-X. Coudert, C. Triguero, A. Boutin, A. H. Fuchs, I. Beurroies and R. Denoyel, *Langmuir*, 2011, **27**, 4734–4741.
5 C. Serre, F. Millange, C. Thouvenot, M. Nogues, G. Marsolier, D. Loueer and G. Férey, *J. Am. Chem. Soc.*, 2002, **124**, 13519–13526.
6 S. Henke, R. Schmid, J.-D. Grunwaldt and R. A. Fischer, *Chem.–Eur. J.*, 2011, **17**, 411.
7 N. Klein, C. Herzog, M. Sabo, I. Senkovska, J. Getzschmann, S. Paasch, M. R. Lohe, E. Brunner and S. Kaskel, *Phys. Chem. Chem. Phys.*, 2010, **12**, 11778–11784.
8 J. Y. Lee, L. Pan, X. Huang, T. J. Emge and J. Li, *Adv. Funct. Mater.*, 2011, **21**, 993–998.
9 D. N. Dybtsev, H. Chun and K. Kim, *Angew. Chem., Int. Ed.*, 2004, **43**, 5033–5036.
10 H. Wang, J. Getzschmann, I. Senkovska and S. Kaskel, *Microporous Mesoporous Mater.*, 2008, **116**, 653–657.
11 P. Maniam and N. Stock, *Inorg. Chem.*, 2011, **50**, 5085–5097.
12 J. Y. Lee, D. H. Olson, L. Pan, T. J. Emge and J. Li, *Adv. Funct. Mater.*, 2007, **17**, 1255–1262.
13 K. S. Walton, A. R. Millward, D. Dubbeldam, H. Frost, J. J. Low, O. M. Yaghi and R. Q. Snurr, *J. Am. Chem. Soc.*, 2008, **130**, 406–407.
14 B. Panella, M. Hirscher, H. Puetter and U. Mueller, *Adv. Funct. Mater.*, 2006, **16**, 520–524.
15 T. Takei, J. Kawashima, T. Ii, A. Maeda, M. Hasegawa, T. Kitagawa, T. Ohmura, M. Ichikawa, M. Hosoe, I. Kanoya and W. Mori, *Bull. Chem. Soc. Jpn.*, 2008, **81**, 847–856.
16 P. Song, Y. Li, B. He, J. Yang, J. Zheng and X. Li, *Microporous Mesoporous Mater.*, 2011, **142**, 208–213.
17 I. Senkovska and S. Kaskel, *Microporous Mesoporous Mater.*, 2008, **112**, 108–115.
18 J. Fraissard and T. Ito, *Zeolites*, 1988, **8**, 350–361.
19 W. Böhlmann, A. Pöppl, M. Sabo and S. Kaskel, *J. Phys. Chem. B*, 2006, **110**, 20177–20181.
20 C.-Y. Cheng, T. C. Stamatatos, G. Christou and C. R. Bowers, *J. Am. Chem. Soc.*, 2010, **132**, 5387–5393.
21 P. J. Barrie and J. Klinowski, *Prog. Nucl. Magn. Reson. Spectrosc.*, 1992, **24**, 91–108.
22 T. Ito and J. Fraissard, *J. Chem. Phys.*, 1982, **76**, 5225–5229.
23 I. Moudrakovski, D. V. Soldatov, J. A. Ripmeester, D. N. Sears and C. J. Jameson, *Proc. Natl. Acad. Sci. U. S. A.*, 2004, **101**, 17924–17929.
24 K. J. Ooms and R. E. Wasylishen, *Microporous Mesoporous Mater.*, 2007, **103**, 341–351.
25 D. Raftery and B. F. Chmelka, *NMR*, 1994, **30**, 111–158.
26 C. I. Ratcliffe, *Annu. Rep. NMR Spectrosc.*, 1998, **36**, 123–221.
27 P. Sozzani, A. Comotti, R. Simonutti, T. Meersmann, J. W. Logan and A. Pines, *Angew. Chem., Int. Ed.*, 2000, **39**, 2695–2698.
28 T. Ueda, K. Kurokawa, T. Eguchi, C. Kachi-Terajima and S. Takamizawa, *J. Phys. Chem. C*, 2007, **111**, 1524–1534.
29 A. Comotti, S. Bracco, P. Valsesia, L. Ferretti and P. Sozzani, *J. Am. Chem. Soc.*, 2007, **129**, 8566–8576.

30 A. Boutin, M.-A. Springuel-Huet, A. Nossov, A. Gedeon, T. Loiseau, C. Volkringer, G. Férey, F.-X. Coudert and A. H. Fuchs, *Angew. Chem., Int. Ed.*, 2009, **48**, 8314–8317.
31 H. C. Hoffmann, B. Assfour, F. Epperlein, N. Klein, S. Paasch, I. Senkovska, S. Kaskel, G. Seifert and E. Brunner, *J. Am. Chem. Soc.*, 2011, **133**, 8681–8690.
32 M.-A. Springuel-Huet, A. Nossov, Z. Adem, F. Guenneau, C. Volkringer, T. Loiseau, G. Férey and A. Gedeon, *J. Am. Chem. Soc.*, 2010, **132**, 11599–11607.
33 A. Lesage, S. Steuernagel and L. Emsley, *J. Am. Chem. Soc.*, 1998, **120**, 7095–7100.
34 E. R. Andrew and A. Jasinski, *J. Phys. C: Solid State Phys.*, 1971, **4**, 391–400.
35 E. Brunner, *J. Chem. Soc., Faraday Trans.*, 1990, **86**, 3957–3960.
36 E. Brunner, *J. Chem. Soc., Faraday Trans.*, 1993, **89**, 165–169.
37 D. Fenzke, B. C. Gerstein and H. Pfeifer, *J. Magn. Reson.*, 1992, **98**, 469–474.
38 D. Schulze, H. Ernst, D. Fenzke, W. Meiler and H. Pfeifer, *J. Phys. Chem.*, 1990, **94**, 3499–3502.
39 F. Gul-E-Noor, B. Jee, A. Pöppl, M. Hartmann, D. Himsl and M. Bertmer, *Phys. Chem. Chem. Phys.*, 2011, **13**, 7783–7788.
40 *STOE WinXPOW Version 1.10*; STOE& Cie GmbH, Darmstadt, Germany, 2002.
41 A. Le Bail, H. Duroy and J. L. Fourquet, *Mater. Res. Bull.*, 1988, **23**, 447–452.
42 J. Rodriguez-Carvajal, in *Abstracts of the Satellite Meeting on Powder Diffraction of the XV Congress of the UCr*, Toulouse, France, 1990.
43 B. M. Fung, A. K. Khitrin and K. Ermolaev, *J. Magn. Reson.*, 2000, **142**, 97–101.

